MICROWAVE SPECTRUM AND DIPOLE MOMENT OF THIONYL TETRAFLUORIDE

by

Patricia Fida Webber

Thesis submitted to the Faculty of the
Virginia Polytechnic Institute and State University
in partial fulfillment of the requirements for the degree of

MASTER OF SCIENCE

in

Chemistry

APPROVED:

J. D. Graybeal, Chairman

J. S. Merola

J. W. Viers

August, 1990
Blacksburg, Virginia

MICROWAVE SPECTRUM AND DIPOLE MOMENT OF THIONYL TETRAFLUORIDE

by

Patricia Fida Webber

Committee Chairman: Jack D. Graybeal
Chemistry

(ABSTRACT)

Electron diffraction and microwave studies of hionyl tetrafluoride (SOF_4) have been conducted in order to determine its molecular structure. The results from these investigations were however found to be inconsistent.

In view of these controversial findings, a microwave investigation was undertaken to accurately assign the rotational transitions, compare the determined moments with those from prior studies and examine the Stark effect in SOF_4 in order to determine its dipole moment.

Calculations using an Asymmetric Rotor program were made to determine the Stark coefficients for transitions having J = 1−40 and frequencies between 12−27 MHz. Absorption peaks were identified as had been predicted by theoretical calculations. The spectrum was very rich and exhibited many strong Q−branch transitions ($\Delta J=0$). Most were high J transitions whose Stark components could not be resolved. The R−branch transitions ($\Delta J=1$), were observable for only low J transitions and at very low Stark voltages.

Stark peaks were not well resolved for the low J transitions; most of them had been masked by the strong Q−branch transitions. Data from the 1(0,1) ----> 2(1,1) transition at 14049 MHz gave a dipole moment of 0.97 Debye.

A least squares fit of the observed frequencies correlated well with those from the structure D4, proposed by Hedberg and Hedberg. The rotational constants and moments of inertia were calculated to obtain the values:

A = 4181.0 ± 0.04 MHz	I_a = 120.9 ± 0.02 amu $\mathring{A}^2$
B = 3289.8 ± 0.04 MHz	I_b = 153.6 ± 0.02 amu $\mathring{A}^2$
C = 3206.3 ± 0.04 MHz	I_c = 157.6 ± 0.02 amu $\mathring{A}^2$

ACKNOWLEDGEMENTS

The author wishes to express her sincere gratitude to her advisor, Dr. J.D. Graybeal for his guidance and support throughout this project both on an official and personal level.

Much thanks also goes to Oksik Jo for her help with the Stark cell as well as her various tutoring and suggestions given throughout various stages of the project.

Dedicated with love and deep appreciation to
Gbenga and the Webber family
(including Mamshu and Clifford).

Thank you for everything and God bless you all.

TABLE OF CONTENTS

LIST OF TABLES

LIST OF FIGURES

INTRODUCTION

Since the first electron diffraction structural investigation by Kimura and Bauer[1] in 1963, controversy regarding the structure of thionyl tetrafluoride (SOF_4) has abounded. These have included: (1) reevaluation of their original work; (2) subsequent electron diffraction studies and a microwave spectroscopic study. The microwave spectrum of this compound was first observed in our laboratory by Shoemaker[2] who assigned a number of Q-branch transitions. Subsequent studies[3] identified what was thought to be a series of R-branch, low J transitions.

This study was undertaken to: (1) Verify the assignment of the low J, R−branch transitions; (2) Obtain a final fit of the spectrum; (3) Determine the dipole moment using the Stark effect of the low J, R-branch transitions and (4) Hopefully settle the controversy as to which of the previous structural studies are valid.

In the course of the investigation, the use of line contours as a means of estimating dipole moment was pursued as an alternate to not having clear, well resolved Stark components.

REVIEW OF PUBLISHED STRUCTURAL STUDIES OF THIONYL TETRAFLUORIDE

Structural information on thionyl tetrafluoride (SOF_4) was first obtained from Raman and Infrared spectra by Goggin, Roberts and Woodward[4], who also studied sulfur tetrafluoride (SF_4). A similarity between the two structures was proposed, with the oxygen atom of SOF_4 in an equatorial position. It was assumed that this position in SF_4 was occupied by a lone pair of electrons. The structure of SF_4 was confirmed by Tolles and Gwinn[5] to have two axial and two equatorial fluorines with C_{2v} symmetry.

In 1963, Kimura and Bauer[1](KB) reported the first study of SOF_4 using electron diffraction. This publication also included work on SF_4. Their report confirmed Goggin et. al's[4] proposed structure of SOF_4 and the similarity to SF_4 for which all four fluorine atoms are on the same side of a plane through the sulfur atom. The axial S−F bonds are approximately 180^o and slightly bent towards the oxygen atom. The equatorial S-F bond distances were determined to be much shorter than the axial S-F bond distances in both structures, with the axial bonds in SOF_4 being about 0.04 A^o shorter than those of SF_4 due to the presence of the oxygen atom. The axial F-S-F angles were found to be greater than 180^o and the equatorial F-S-F angles greater than 120^o for SOF_4. Figures 1 and 2 show the electron diffraction structures of SF_4 and SOF_4 respectively. Hencher, Cruickshank and Bauer[6](HCB) later reexamined the data and proposed two different conformations of SOF_4, I and II, with axial and equatorial FSF angles less than 180^o and 120^o degrees respectively. Structure II was preferred because it was more consistent with Gillespie's predictions, using the VSEPR theory[7].

Additional electron diffraction studies by Gundersen and Hedberg[8] (GH) reported four possible conformational structures, A, B, C and D; structure B was preferred because it was in better agreement with those of HCB[6]. In 1982, Hedberg and Hedberg[9] (HH) published additional information that supported a D type instead of a B type model because vibrational effects, when taken into consideration, gave results that correlated very well with the calculated parameters. Refer to Table 1 for the structural data by GH, HCB and HH.

An early microwave spectroscopic study of the compound was conducted by Murty[10] but resulted in a misassignment of the spectrum as the study could not be repeated and none of the calculated parameters were close in value to those predicted by electron diffraction.

In view of these controversial results, a microwave investigation of thionyl tetrafluoride

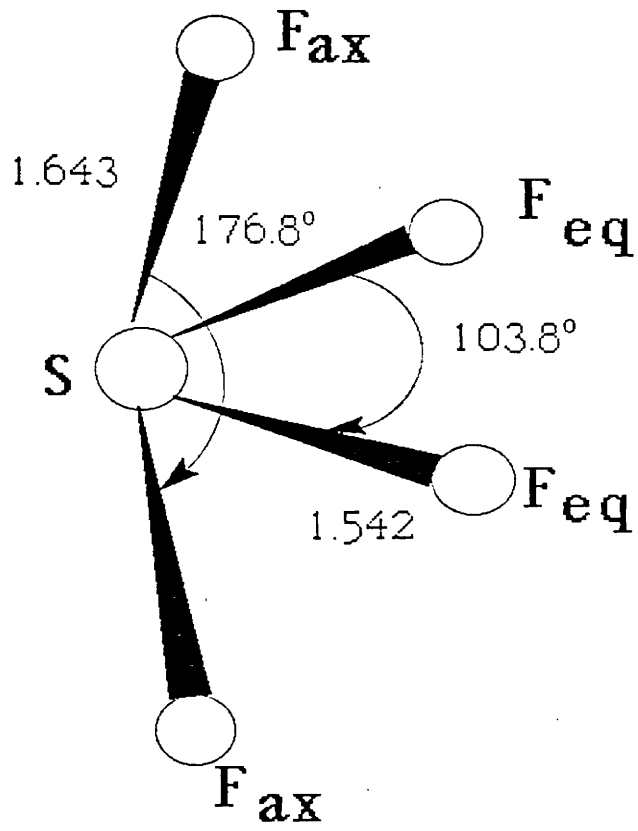

Figure 1: Electron Diffraction Structure of SF_4

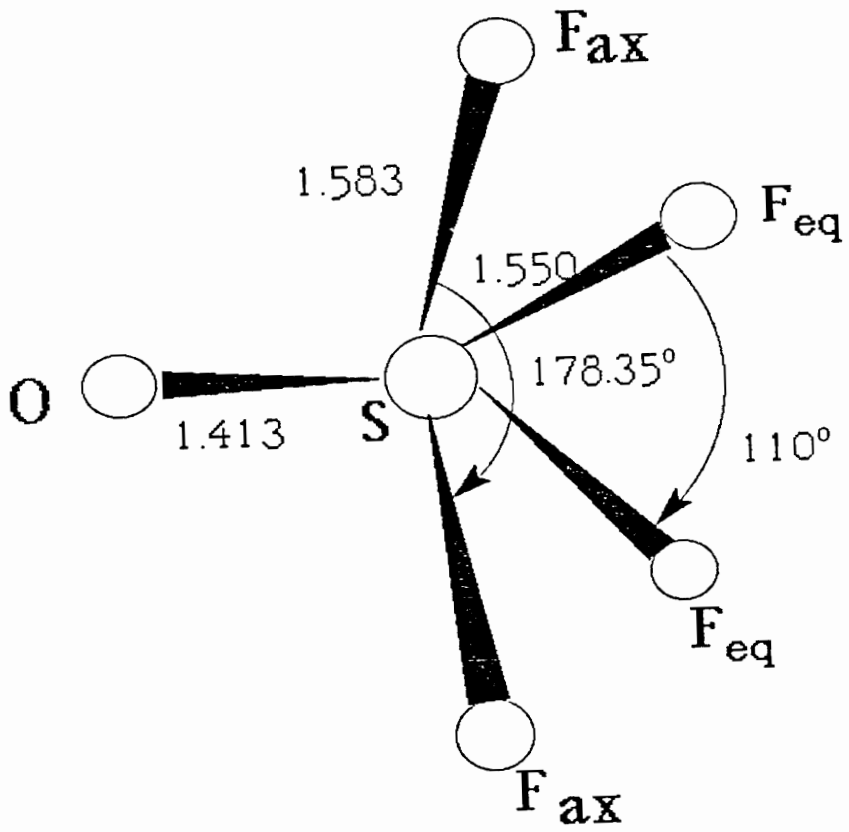

Figure 2: Representative Electron Diffraction Structure of SOF_4

was undertaken in order to accurately assign the rotational transitions to verify the electron diffraction structure and to examine the Stark effect on SOF_4 and determine its dipole moment.

Table 1

Structural Parameters for SOF_4 from Electron Diffraction Data

	GH[a]−A	GH−B	GH−C	GH−D
r_SO	1.402	1.403	1.406	1.405
r_SF(eq)	1.548	1.552	1.535	1.533
r_SF (ax)	1.578	1.575	1.593	1.596
< FSF (eq)	117.92	110.17	118.74	114.92
<F(ax)SO	90.60	90.65	98.03	97.77
< F (ax) SF (eq)	89.69	89.63	85.92	85.83
< F(eq) SO	121.04	124.91	120.63	122.54
< FSF(ax)	NR	NR	NR	NR
Rot. Const.				
A	4145.335	4146.538	4173.996	4199.940
B	3376.459	3269.459	3384.305	3327.341
C	3130.275	3243.924	3142.302	3188.946

a= Gundersen and Hedberg[8] (Structures A, B, C, D)

NR= Not Reported

Table 1 (contd.)

Structural Parameters for SOF_4 from Electron Diffraction Data

	HCB[b] – I	HCB – II	HH – D4
r_SO	1.413	1.413	1.409
r_SF(eq)	1.550	1.550	1.539
r_SF (ax)	1.582	1.583	1.596
< FSF (eq)	119.4	110.01	112.8
< F(ax) SO	91.05	90.82	97.71
< F(ax)SF(eq)	89.50	89.49	85.71
< F(eq) SO	120.3	124.99	123.62
< FSF(ax)	182.8	178.35	NR
Rot. Const.			
A	4118.473	4139.937	4179.068
B	3375.410	3239.591	3291.424
C	3098.302	3229.943	3209.060

b= Hencher, Cruickshank and Bauer[6] (Structures I and II)

c= Hedberg and Hedberg[9]

NR= Not Reported

THEORETICAL ASPECTS

Microwave spectroscopy studies the pure rotational spectra of gaseous molecules. It covers a frequency range of 3–300 GHz. Spectral lines arise from transitions between quantized rotational energy levels, separated by $\Delta E = h\nu$, where ν is the frequency of the microwave radiation. Rotational transitions are produced by electric dipole coupling.

From an analysis of the observed spectra and the correct assignment of the transitions, a molecular structure can be determined. Molecules are classified based on their moments of inertia, I_a, I_b, I_c, where the a, b and c axes are with respect to the x, y, and z axes respectively. Table II shows this classification of molecules. From the electron diffraction work done on SOF_4, it is expected that it will be an asymmetric top molecule with only c-dipole (μ_c) type transitions.

Following is a summary of the theoretical aspects of use in this investigation.

Table 2

Molecular Classification According to Moments of Inertia

Types of Rotors: Rotor	Principal Moments ofInertia	Examples
Linear	$I_a\ (\approx 0) < I_b = I_c$	HCl, OCS
Spherical	$I_a = I_b = I_c$	SiH_4, CH_4
Prolate Symmetric	$I_a < I_b = I_c$	NH_3, POF_3
Oblate Symmetric	$I_a = I_b < I_c$	$CHCl_3$, C_6H_6
Asymmetric	$I_a \neq I_b \neq I_c$	BF_2OH, F_2CO

ASYMMETRIC ROTORS

The rotational spectrum of an asymmetric top molecule is very complex because none of its principal moments of inertia is zero and no two are equal. That is, $I_a \neq I_b \neq I_c$. Conventionally, $I_a < I_b < I_c$, where a, b and c are the principal inertial axes. Molecular asymmetry can be characterized by Ray's asymmetry parameter[11]

$$\kappa = \frac{2B - A - C}{A - C} \tag{1}$$

where A, B and C are the rotational constants and are defined as

$$A = \frac{h^2}{8\pi^2 I_a} \tag{2}$$

$$B = \frac{h^2}{8\pi^2 I_b} \tag{3}$$

$$C = \frac{h^2}{8\pi^2 I_c} \tag{4}$$

Ray's parameter, κ, lies between the limits of $+1$ and -1. When $\kappa \approx -1$, I_b-----> I_c and a prolate symmetric top is approached; conversely, when $\kappa \approx +1$, I_b---->I_a and an oblate symmetric top is approached. The energy levels of asymmetric rotors differ from the limiting symmetric rotors in that the levels corresponding to non-zero values of K are separated. The levels are indexed by subscripting the J value of a given rotational level with pseudo quantum numbers, K_{-1} and K_{+1} which relate to the symmetric rotor limits. This non-degeneracy introduces $(2J+1)$ distinct rotational sub-levels for each J value. The first number, K_{-1}, represents the K value for the limiting prolate rotor while K_{+1} represents the K value of the limiting oblate symmetric rotor. Table 3 shows the selection rules for an asymmetric rotor.

Table 3

Selection Rules for an Asymmetric Rotor			
μ_g (g = a, b, c)	ΔJ	ΔK_{-1}	ΔK_{+1}
μ_a	0, ± 1	0, ± 2, ...	±1, ±3, ...
μ_b	0, ± 1	± 1, ± 2, ...	± 1, ± 3, ...
μ_c	0, ± 1	± 1, ± 3, ...	0, ± 2, ...

ENERGIES OF ASYMMETRIC MOLECULES

The rotational wave functions and their attendant energies can be determined from the eigenvalue equation

$$\mathcal{H}_r \ \psi_i = E_i \ \psi_i \tag{5}$$

$\mathcal{H}_r$ is the quantum mechanical operator corresponding to the classical rotation as defined by

$$\mathcal{H}_r = \frac{1}{2}\left(I_x \ \omega_x^2 + I_y \ \omega_y^2 + I_z \ \omega_z^2 \right) \tag{6}$$

where I_x, I_y and I_z are the principal moments of inertia and ω_x, ω_y and ω_z are the cartesian components of the angular velocities in the principal inertial axis system.
The principal moments of inertia are defined as

$$I_x = \sum_i^N m_i \left(y_i^2 + z_i^2 \right) \tag{7}$$

$$I_y = \sum_i^N m_i \left(x_i^2 + z_i^2 \right) \tag{8}$$

$$I_z = \sum_i^N m_i \left(x_i^2 + y_i^2 \right) \tag{9}$$

The angular momentum is related to the angular velocity by

$$P_g = I_g \ \omega_g \qquad (g = x, y, z) \tag{10}$$

Therefore the classical rotational energy can be written in terms of angular momentum

$$H = \frac{1}{2}\left(\frac{P_x^2}{I_x} + \frac{P_y^2}{I_y} + \frac{P_z^2}{I_z} \right) \tag{11}$$

and the quantum mechanical expression is

$$\mathcal{H}_r = \frac{1}{2}\left(\frac{P_x^2}{I_x} + \frac{P_y^2}{I_y} + \frac{P_z^2}{I_z} \right) \tag{12}$$

where the classical angular momenta have been replaced by angular momentum operators, P_x, P_y and P_z. They are defined as

$$P_x = \frac{ih}{2\pi}\left(z\frac{\delta}{\delta y} - y\frac{\delta}{\delta z} \right) \tag{13}$$

$$P_y = \frac{ih}{2\pi}\left(x\frac{\delta}{\delta z} - z\frac{\delta}{\delta x} \right) \tag{14}$$

$$P_z = \frac{ih}{2\pi}\left(y\frac{\delta}{\delta x} - x\frac{\delta}{\delta y} \right) \tag{15}$$

A review of the methods used for the determination of the energy levels for an asymmetric rotor are available in several sources.[11,12]

The eigenvalues of the Hamiltonian operator are the quantized energies from which the microwave spectral frequencies are determined. Due to the splitting in the K levels, the Hamiltonian will be non-diagonal for an asymmetric rotor. Therefore, a transformation must be found which will diagonalize $\mathcal{H}_r$. One can make use of the matrix elements of the angular momentum when solving for the energy levels. The elements of the Hamiltonian matrix are given by

$$\left(J, K, M \mid \mathcal{H}_r \mid J', K', M' \right) = \frac{1}{2}\left(J, K, M \mid \frac{P_x^2}{I_x} + \frac{P_y^2}{I_y} + \frac{P_z^2}{I_z} \mid J', K', M' \right) \tag{16}$$

where

J= quantum number specifying the total angular momentum. (J = 0, 1, 2, ...)

K= quantum number specifying the component of the angular momentum about the molecular symmetry axis. (K = J, J−1, J−2, ··· ··· ···, −J)

M= quantum number specifying a component of angular momentum about a space fixed z- axis.

$$(M = J, J-1, J-2, \cdots \cdots \cdots, -J)$$

The squared angular momentum operators can be expressed by the matrix product rule

$$\left(J, K, M \mid P_g^2 \mid J',K',M' \right) = \sum_{J''K''M''} \left(J, K, M \mid P_g \mid J'',K'',M'' \right)\left(J'',K'',M'' \mid P_g \mid J',K',M' \right) \quad (17)$$

The above equation gives rise to the matrix element for P_x^2, P_y^2 and P_z^2, given in Table IV. Substitution of these equations into equation (6) for the Hamiltonian operator, gives the non-zero terms for an asymmetric rotor

$$(J, K, \mid \mathfrak{H}_r \mid J, K) = \frac{h^2}{16\pi^2} \left(J(J+1) \left\{ \frac{1}{I_x} + \frac{1}{I_y} \right\} + K^2 \left\{ \frac{2}{I_z} - \frac{1}{I_x} - \frac{1}{I_y} \right\} \right) \quad (18)$$

and

$$(J, K, M \mid \mathfrak{H}_r \mid J, K\pm2, M = \frac{h^2}{32\pi^2} \sqrt{\Big(J(J+1) - K(K\pm1) \Big)}$$

$$\times \sqrt{\Big(J(J+1) - (K\pm1)\,(K\pm 2) \Big)} \quad \left(\frac{1}{I_y} - \frac{1}{I_x} \right) \quad (19)$$

Equation (17) gives the diagonal elements of $\mathfrak{H}_r$ while equation (18) gives the off diagonal elements in K. Note that the diagonal elements do not depend on M and that the Hamiltonian matrix elements vanish unless

$$J', M' = J, M$$
$$K' = K, K\pm2$$

Therefore, there are no off diagonal elements in J or M (the energy is independent of the spatial

orientation of P) and the matrices can be treated separately, since they are independent. This will give rise to a secular determinant to be solved for each value of J. Since K takes on all integral values from $-J$ to $+J$, each determinant will be of order $(2J + 1)$.

To set up the energy matrix, it is first necessary to find the non-zero elements of the Hamiltonian[11,12]

$$\mathcal{H}_r = \tfrac{1}{2}(A + C)P^2 + \tfrac{1}{2}\left(A - C\right)\mathcal{H}(\kappa) \tag{20}$$

where the reduced Hamiltonian, $\mathcal{H}(\kappa)$, is defined as

$$\mathcal{H}(\kappa) = P_a^2 + \kappa P_b^2 - P_c^2 \tag{21}$$

and

$$P^2 = P_{a(x)}^2 + P_{b(y)}^2 + P_{c(z)}^2 \tag{22}$$

The energy matrix elements are given in Table 4 and is of the form

$$| E(\kappa) - I\lambda | = 0 \tag{23}$$

where

$E(\kappa)$ = the reduced energy matrix
λ = the allowed energy levels (eigenvalues) for an asymmetric rotor
I = unit matrix

The total rotational energy for a particular level is given by

$$E = \tfrac{1}{2}(A + C)J(J+1) + \tfrac{1}{2}(A - C)E_{J,\tau}(\kappa) \tag{24}$$

The non-zero elements of $E(\kappa)$ are

$$E_{K,K} = \left(J, K, M \mid \mathcal{H}(\kappa) \mid J, K, M\right) = F\left(J(J+1) - K^2\right) + G K^2 \tag{25}$$

and

$$E_{K,K\pm2} = \left(J, K, M \mid \mathfrak{H}(\kappa) \mid J, K\pm2, M\right) = H\, f\sqrt{\left(J, K\pm1\right)} \tag{26}$$

where

$$f = \left(J, K\pm1\right) = \tfrac{1}{4}\left(J\,(J+1) - K\,(K\pm1)\right)\left(J\,(J+1) - (K\pm1)\,(K\pm2)\right) \tag{27}$$

Take into consideration that

$$E_{-k,-k} = E_{k,k} \qquad E_{k,k+2} = E_{k+2,k} = E_{-k,-k-2} = E_{-k-2,-k}$$

The values for the constants F,G and H depend on how the a, b and c axes are identified with the x, y and z axes and there are six possible ways to make this identification[12].

Table 4

The Angular Momentum Energy Matrix Elements
$\left(J, K, M \mid P_z \mid J, K, M\right) = \frac{h}{2\pi} K$
$(J, K, M \mid P_y \mid J, K, M) = \mp i \frac{h}{2\pi} (J, K, M \mid P_x \mid J, K, M)$ $= h \left(\frac{1}{4\pi}\right) \left(J(J+1) - K(K \pm 1)\right)$
$(J, K, M \mid P^2 \mid J, K, M) = \frac{h^2}{4\pi^2} J(J+1)$
$(J, K, M \mid P_z^2 \mid J, K, M) = \frac{h^2}{4\pi^2} K^2$
$(J, K, M \mid P_x^2 \mid J, K, M) = (J, K, M \mid P_y^2 \mid J, K, M) = \frac{h^2}{8\pi^2} \left(J(J+1) - K^2\right)$
$\left(J, K, M \mid P_x^2 \mid J, K, \pm 2, M\right) = -(J, K, M \mid P_y^2 \mid J, K \pm 2, M)$ $= \frac{h^2}{8\pi^2} \sqrt{J(J+1) - K(K \pm 1)}$ $\times \sqrt{J(J+1) - (K \pm 1)(K \pm 2)}$

THE STARK EFFECT

The presence of a dipole moment causes an interaction between a static electric field and a rotating molecule. When the electric field perturbs the molecule's energy levels due to this interaction, the phenomenon is known as the Stark effect. The Stark effect is very useful in microwave spectroscopy as a means for aiding in the assignment of pure rotational lines, especially asymmetric-top molecules. It also provides a method for the determination of the molecular electric dipole moment in the gaseous phase where solvent effects do not perturb the measurement. From the selection rules, J and M values can be estimated to aid in the assignments, from which the dipole moment can then be determined.

The Stark effect selection rules for M depend upon the orientation of the microwave radiation and the electric Stark field, ϵ. If the applied Stark field is parallel to the radiation frequency field, then $\Delta M = 0$ (π components); if the fields are perpendicular, then $\Delta M = \pm 1$ (σ components). In this study, a parallel field was applied. Thus, for R−branch transitions, J + 1 Stark components will be observed (where $J = J_{min}$). Also, the larger intensity corresponds to the smallest M value. For Q−branch transitions, only J Stark components will be observed because the M = 0 transition disappears. In this case, the larger intensity corresponds to the largest M value.

A molecule's dipole moment can be determined from the frequency shift, $\Delta\nu_M$, between the Stark frequency and the absorption frequency. The relationship is

$$\Delta\nu_M = \sum_g (A_g + B_g M^2) \epsilon^2 \mu_g^2 \qquad (g = a, b, c) \qquad (28)$$

where A and B are constants whose values depend on the moments of inertia and the quantum numbers of the energy levels and determine in which direction the Stark components are shifting with increasing field strength. If A and B both have the same sign, then the largest Stark displacement from the unperturbed line will correspond to the largest M value. The dipole moment can be found by plotting a graph of $\Delta\nu$ versus ϵ^2 and determining the slope. SOF_4 has only a μ_c type transition because the dipole lies only along the c-axis (lying parallel to the S=O bond), therefore, $\mu = \mu_c$.

EXPERIMENTAL ANALYSIS OF SOF_4

SOF_4 was obtained from Dr. Joe Thrasher at the University of Alabama and was prepared by the reaction of thionyl fluoride with fluorine gas.

$$SOF_2 + F_2 \text{-------} > SOF_4$$

Mass spectral analysis indicates the presence of small amounts of SF_6 and SO_2F_2 as impurities. These impurities are not detrimental to the study since SF_6 has no rotational spectrum due to the symmetry and the SO_2F_2 rotational spectrum has been well characterized, having only ten observed transitions between 12 and 26 GHz, these being clustered between 20218 and 20260 MHz. Since the melting and boiling points of SOF_4 were -99.6^oC and -49.0^oC respectively, its microwave spectrum was run at temperatures between -10^oC and -40^oC by cooling the cell with dry ice. This helps to increase the population of the lower energy levels as well as reduce noise in the detector.

The study was done using a Stark modulated spectrometer in the frequency range of 12−26 GHz. Figure 3 shows a block diagram of a Stark modulated spectrometer. The spectrometer source was a Hewlett Packard Model 8673B synthesized signal generator, covering a frequency range from 2−26 GHz. The detector was a crystal diode rectifier. Its output was fed to a pre-amplifier and then to an E, G & G Model 5207 lock-in amplifier where the signal from the amplifier was compared to a signal from the modulation source. This method provides narrow-band amplification over a wide frequency range. The data can then be read from the digital display or sent to a computer. Also a Fisher Recordall Series 5000 chart recorder can be used to display the conventional spectrum.

The Hewlett Packard Model 220S computer is used instead of the chart recorder for more accurate measurements. Data was stored in the computer using a BASIC 2.1 Operating System.

The Stark cell was calibrated using carbonyl sulfide (OCS), with a known dipole moment of 0.71521 D.

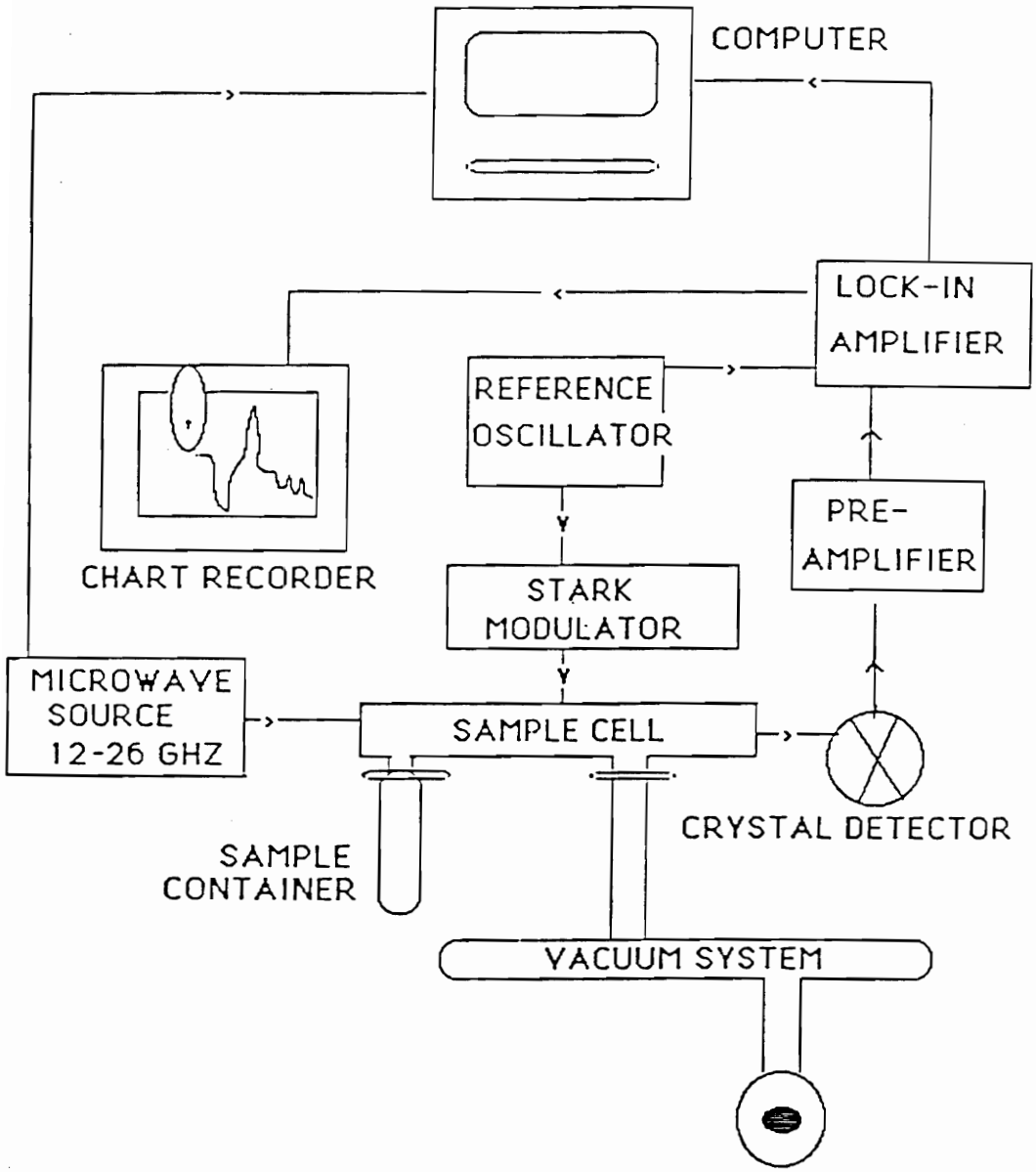

Figure 3: Schematic Diagram of the Stark Modulated Spectrometer

EXPERIMENTAL RESULTS AND OBSERVATIONS

Being an asymmetric molecule, with μ_C type transition, the selection rules for the rotational transitions of SOF_4 are:

$$\Delta K_{-1} = \pm 1, \pm 3$$

$$\Delta K_1 = 0, \pm 2$$

$$\Delta J = 0, \pm 1$$

From an earlier microwave investigation[2] several Q ($\Delta J = 0$) and R ($\Delta J = 1$) branch transitions had been observed and assigned but their Stark effects had not been examined. Calculations using an Asymmetric Rotor Program[14] were made in order to determine the Stark coefficients for transitions having J=1−40 and frequencies between 12−27 MHz.
The calculations provided the coefficients for the Stark shift equation

$$\Delta\nu = (A_c + B_c M^2)\, \mu_c^2\, \epsilon^2 \qquad (29)$$

The following rotational constants taken from Hedberg and Hedberg[9] were used in this calculation.

A = 4181.040 B = 3289.840 C = 3206.300 κ = -0.828590188

The values of A and B did not change much for each electron diffraction data set.

The SOF_4 spectrum was very rich and exhibited many Q−branch transitions. These Q-type transitions became dominant at high Stark voltages ($\geq$ 200V). Most were high J transitions whose Stark components could not be resolved. By assuming that the maximum of the Stark lines for a given Q−branch transition corresponded to the most intense component and calculating the Stark shifts as a function of the dipole moment, it was estimated that the dipole moment would lie between 0.9 D and 1.2 D.

R branch transitions were observable for only low J values and at very low Stark voltages ($<$ 300V). It was expected that the Stark peaks would be very well resolved for the low J transitions but it was found that most of them were masked by the strong Q−branch transitions. The strongest transitions were observed between 25V and 100V.

THEORETICAL CALCULATION OF LINE SHAPES USING LINE WIDTH DATA

The conventional method used for the determination of the dipole moment is to plot the Stark splittings versus the square of the electric field strengths and extract μ from the slope of the linear plot. In the present study it was found that the richness of the spectrum, relative to Q−branch transitions at electric field strengths as low as 400v/cm obliterate the Stark components of the low J (< 3), R−branch transitions. This necessitated use of Stark components which were only minimally shifted from the transitions for determination of μ. In these cases the plots of $\Delta\nu$ versus ϵ^2 were non linear at the low fields. This nonlinearity was determined not to be due to degeneracy effects as was first suspected but rather to line distortion resulting from the magnitude of the line widths and close proximities of the unsplit lines and its Stark components. This problem has been examined in some detail and a program was developed to relate the observed splittings to the line width, field strengths and dipole moments. Use of this information may have the capability for estimation of dipole moments from observed line contours but that aspect has not been pursued except for a few molecules exhibiting $J < 14$ Q−branch transitions.

For low J transitions where a resolved Stark pattern can be obtained, a direct count of each M_J component can be made. There will be a maximum of (J+1) Stark components when $\Delta J = \pm 1$, and J components when $\Delta J = 0$, where each corresponds to an M_J value. Also, the maximum value of M_J corresponds to the smaller J value. For a low J transition, where the Stark shift is large and therefore shows resolved Stark shifts, the Stark effect will be of the form given in Figure 4. The figure shows the case for a $J = 2$ transition, with $J+1 = 3$ Stark components. The total intensity of all the Stark components is always equal to that of the unsplit line; also the line width of the unsplit line and each of the Stark components is the same, $2\underline{\Delta\nu}$.

For SOF_4 the high J transitions experience very small Stark shifts and the overall pattern is usually of the form in Figure 5, indicating the unsplit line with all of its Stark components overlapping each other. As a result, what resembles a single Stark peak is observed for a transition like Figure 6 where

ν_{0k} = unsplit transition, k = J

ν_{ikl} = i^{th} Stark component for transition k at electric field, ϵ_l

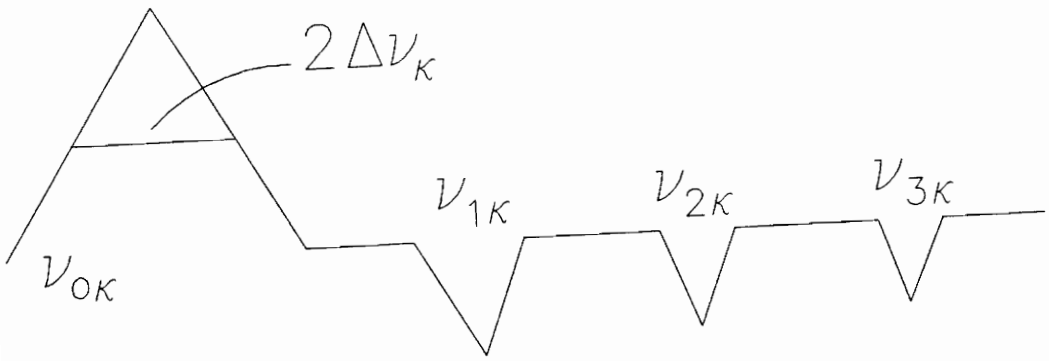

Figure 4: Resolved Stark shifts for a low J transition

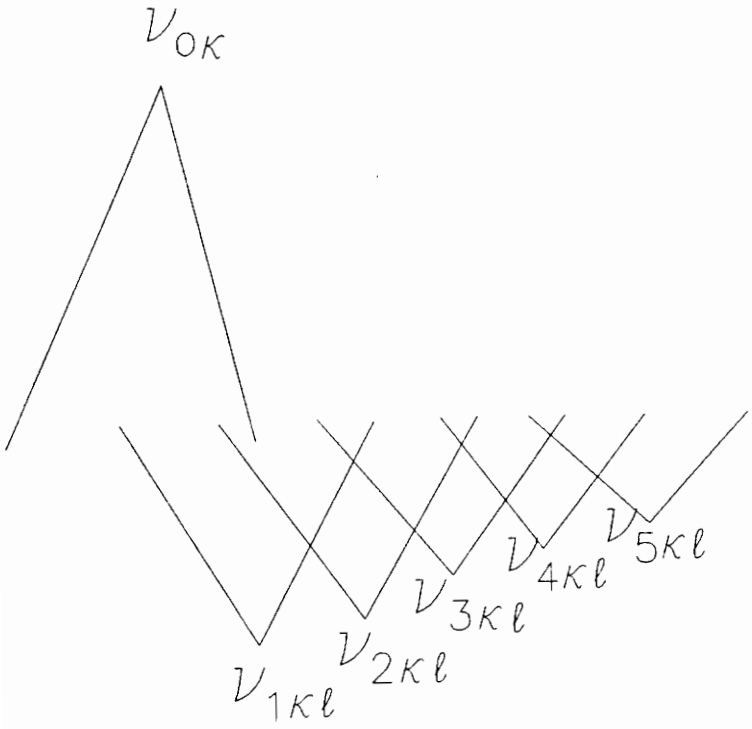

Figure 5: Overall pattern for a high J transition

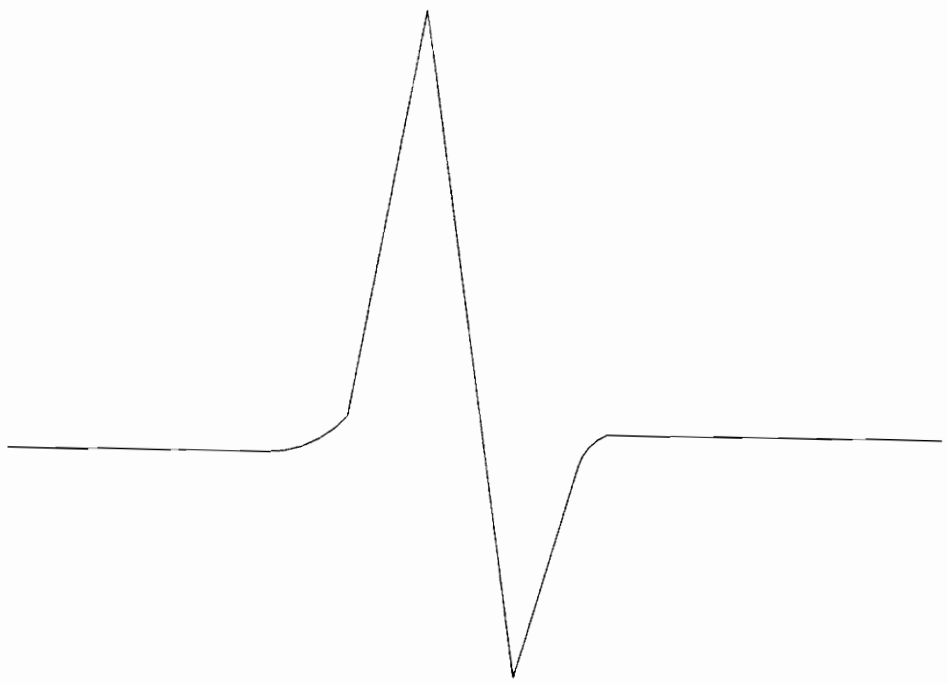

Figure 6: Schematic of observed pattern for a high J transition

The overall line shape is given by the equation

$$S_{kl}(\nu_j) = S_{0k}(\nu_j) - \sum_{i=1}^{J+1} S_{ikl}(\nu_j) \qquad (30)$$

where

$S_{0k}(\nu_j)$ = shape function of the unsplit line for transition k as a function of frequency, ν_j.

$S_{ikl}(\nu_j)$ = shape function of the i^{th} Stark component of transition k at electric field, ϵ_l.

Assuming a Lorentzian line shape because a low pressure was used, $\Delta\nu_k << \nu_{0k}$ and the above functions can be given by

$$S_{0k}(\nu_j) = I_k\left(\frac{\underline{\Delta\nu_k}}{(\underline{\Delta\nu_k})^2+(\nu_j-\nu_{0k})^2}\right) \qquad (31)$$

$$S_{ikl}(\nu_j) = L_{ik}\left(\frac{\underline{\Delta\nu_{ik}}}{(\underline{\Delta\nu_{ik}})^2+(\nu_j-\nu_{ikl})^2}\right) \qquad (32)$$

where

$\underline{\Delta\nu_k}$ = half width at half height of the k^{th} unsplit transition

L_{ik} = intensity factor for the i^{th} Stark component of the k^{th} transition

$I_k = \sum_{i=1}^{2J+1} L_{ik}$ = the intensity factor for the unsplit transition, ν_{0k}

ν_{ikl} = frequency of the i^{th} Stark component of transition at ϵ_l

ν_j = incremental values of frequencies

For a given Stark pattern, the frequency spread would run from ($\nu_{0k}-4\Delta\nu_k$) to ($\nu_{J+1}+4\Delta\nu_k$), with incremental values of ν_j such that the step size, $\nu_{j+1}-\nu_j$ is small enough to give 100 points over the frequency range of $2\Delta\nu$. The frequency, ν_{J+1} is that of the Stark component with the largest displacement from the absorption peak.

Since the total line shape depends upon the splitting of the Stark components, which in turn depends upon μ and ϵ, the value of ν_{ikl} can therefore be determined by rearranging the Stark shift equation, from which the frequency of the i^{th} Stark component of transition ν_{0k} will be given by

$$\nu_{ikl} = \nu_{0k} + \left(A_k + B_k M_{ik}^2\right) \mu^2 \epsilon_l^2 \qquad (33)$$

where A_k and B_k are the same values used in the Asymmetric Rotor calculations and

$$\begin{aligned} L_{ik} &= M_{ik}^2 && \Delta J = 0 \\ &= \left\{(J+1)^2\right\} - M_{ik}^2 && \Delta J = \pm 1 \end{aligned}$$

The shape function can then be determined by substituting equation (33) back into the denominator of equation (32) and then (31) and (32) back into equation (30). By varying the μ and ϵ_l, the overall line shape can then be calculated to give a contour similar to the observed transition.

DISCUSSION OF LINE SHAPE ANALYSIS

In order to perform the calculations, a program was written in the Dbase language that would determine S_{kl} for every step, so that a plotted curve could be derived. The program was written such that by varying the dipole moments, S_{kl} values can be calculated for a series of electric fields. Previous calculations had suggested the dipole moment to be between 0.5 and 1.5 Debye; also, the values of the electric field were those due to applied voltages of 25 to 1200 V. In short, for each dipole moment, a range of S_{kl} values will be derived for every value of the electric field. From the data retrieved, the S_{kl} and ν_j values can then be plotted to produce the curve with the dipole moment that most closely resembles the experimental one. The data used were:

Dipole Moment Values (D)	Voltage (V)	Electric Field (V/cm)
0.5	25	85
0.7	50	155
1.0	100	294
1.3	150	433
1.5	200	572
	400	1144
	600	1651
	800	2207
	1000	2762
	1200	3318

Calculations were only made for the low J transitions and the results plotted using the Lotus 1-2-3 program. For each dipole moment, there were ten sets of output data corresponding to the ten electric fields used. The plotted output data did not give as much information as was expected but it did show the effect of line width on Stark separation. The calculated Stark peaks were more pronounced for μ = 1.0 and 1.3, with the strongest intensities above 600V.

For illustration, consider the J = 2_{02} ----> 3_{12} transition calculated at 20673 MHz, for which three Stark peaks were expected. Figures 7−9 show line shapes for μ= 1.0 D while Figures 10−12 show the line shapes for μ= 1.3 D. Calculated line shapes for the range of 400 − 1200 V for both dipole values show increasing prominence of the Stark peaks and decreasing line width

with increasing field strength. The data goes further to show that for the same range of voltages, the third Stark peak only begins to show at 800V for $\mu =$ 1.0 D while it is already observable at 600V for $\mu =$ 1.3 D.

For the high J transitions, there is no resolution of the Stark components so dipole moments were estimated by assuming that the maximum Stark peak occurs for the M_{max}=J component. A comparison with experimental data provided estimates of the dipole moment as shown in Table 5. For the transitions, the average value of the dipole moment, $\mu_{av} =$ 1.1 D. This is certainly a reasonable estimate in light of the value of $\mu =$ 0.97 D found using the Stark shift for the 1_{01}----->2_{11} transition at 14049.225 MHz (discussion to follow).

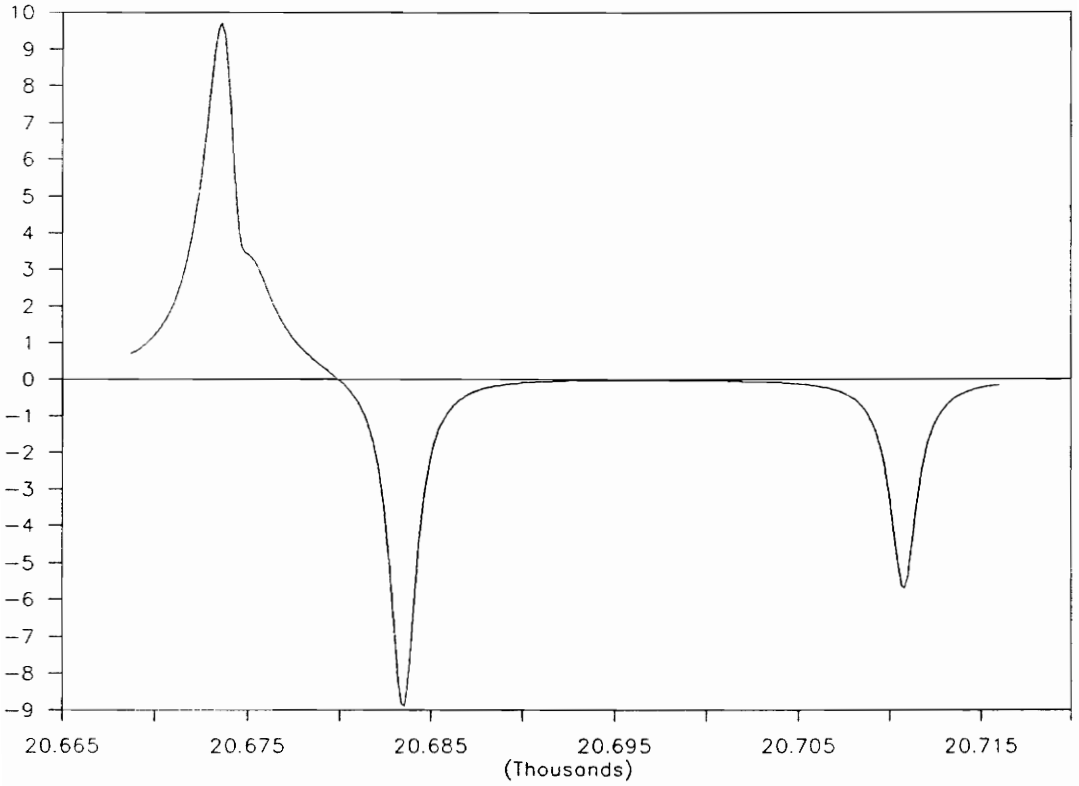

Figure 7: Line Shape at 600V and $\mu = 1$ D

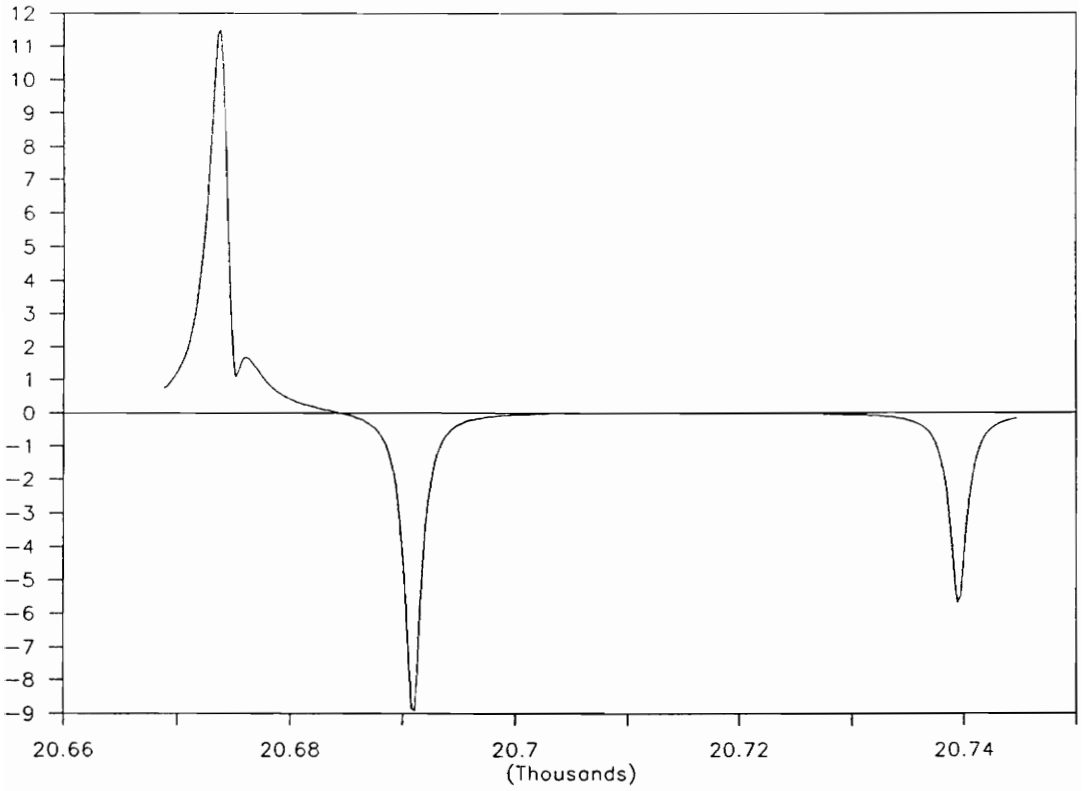

Figure 8: Line Shape at 800V and $\mu = 1$ D

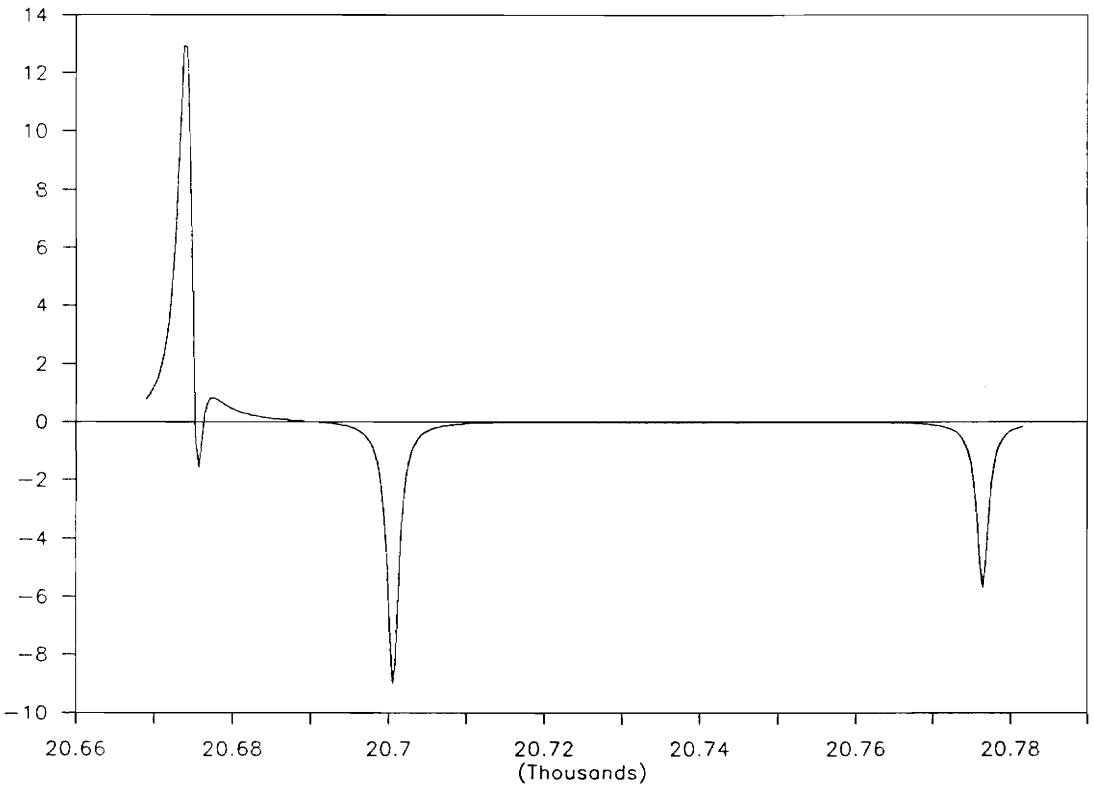

Figure 9: Line Shape at 1000V and $\mu = 1$ D

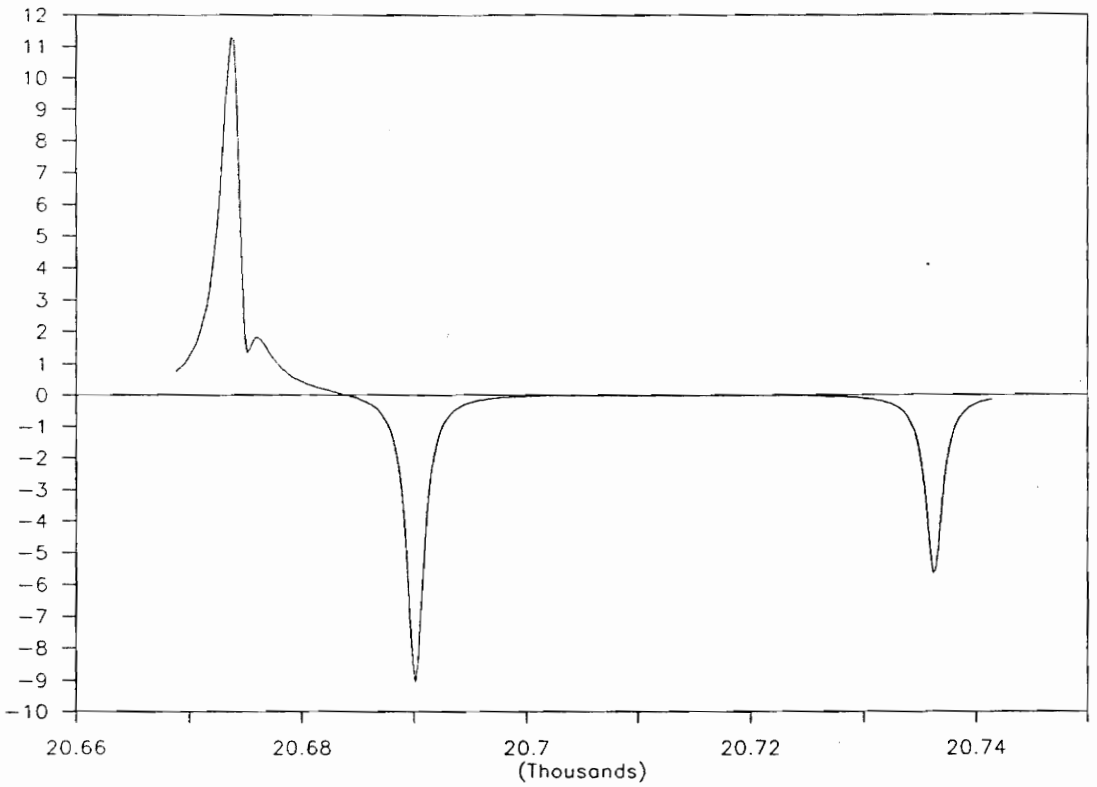

Figure 10: Line Shape at 600V and μ= 1.3 D

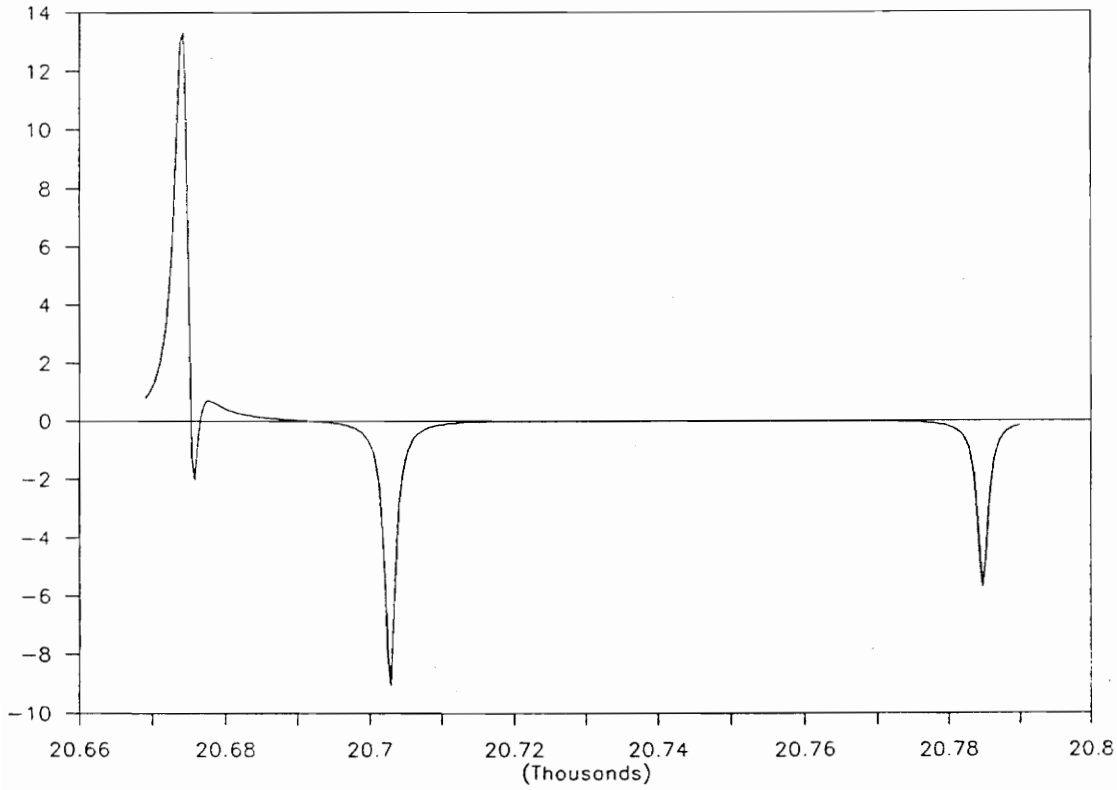

Figure 11: Line Shape at 800V and $\mu = 1.3$ D

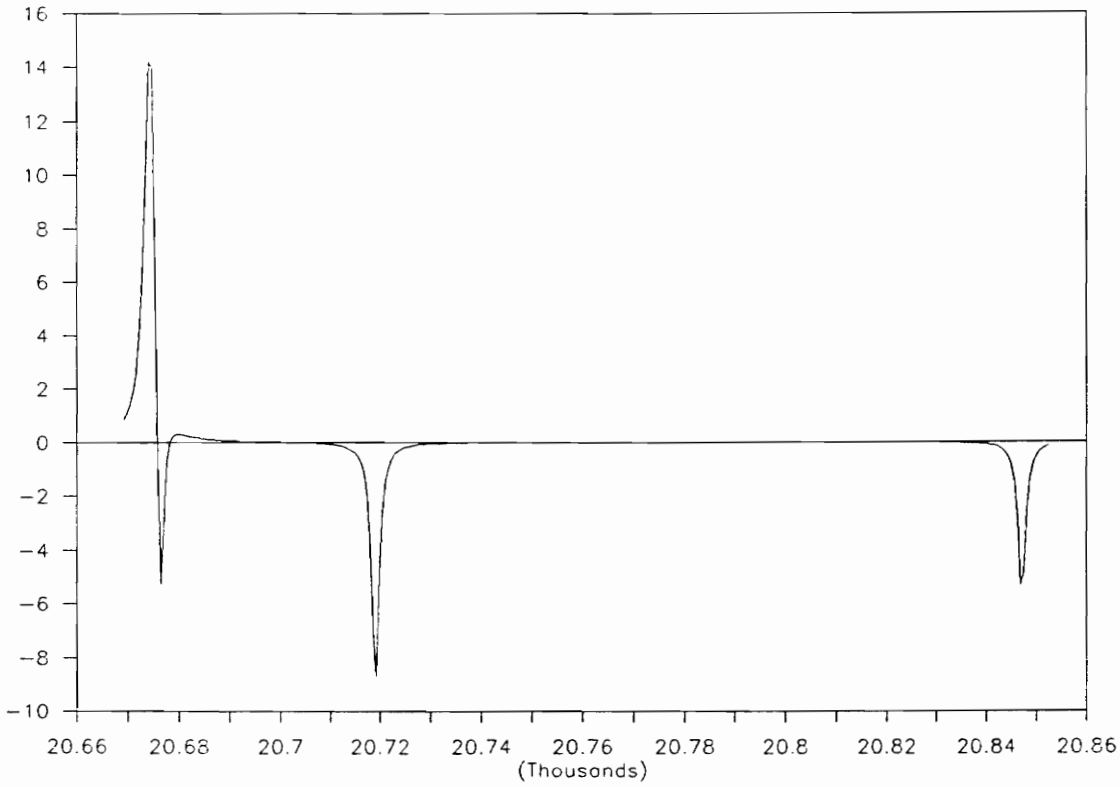

Figure 12: Line Shape at 1000V and $\mu =$ 1.3 D

Table 5

Estimated Dipole Moment from Composite Stark Peak Maximum

Transition	Absorption Peak (MHz)	Estimated μ (Debye)
$^{8}{}_{8,0} - {}^{8}{}_{7,2}$	13977.684	1.126
$^{10}{}_{10,0} - {}^{10}{}_{9,2}$	17705.397	1.444
$^{10}{}_{8,2} - {}^{10}{}_{7,4}$	13969.596	0.992
$^{10}{}_{9,1} - {}^{10}{}_{8,3}$	15838.668	1.024
$^{11}{}_{10,1} - {}^{11}{}_{9,3}$	17702.565	1.126
$^{11}{}_{8,3} - {}^{11}{}_{7,5}$	13963.797	0.967
$^{11}{}_{9,2} - {}^{11}{}_{8,4}$	15834.372	0.857
$^{12}{}_{10,2} - {}^{12}{}_{9,4}$	17698.833	1.142
$^{12}{}_{8,4} - {}^{12}{}_{7,6}$	13955.880	1.021
$^{12}{}_{9,3} - {}^{12}{}_{8,5}$	15828.969	0.948
$^{13}{}_{10,3} - {}^{13}{}_{9,5}$	17694.198	1.227
$^{13}{}_{8,5} - {}^{13}{}_{7,7}$	13945.869	1.075
$^{13}{}_{9,4} - {}^{13}{}_{8,6}$	15822.324	1.349
$^{14}{}_{10,4} - {}^{14}{}_{9,6}$	17688.102	1.367
$^{14}{}_{8,6} - {}^{14}{}_{7,8}$	13932.978	1.167
$^{14}{}_{9,5} - {}^{14}{}_{8,7}$	15813.765	0.955

Estimated Average = 1.1 D

SPECTRAL ASSIGNMENT AND DIPOLE MOMENT DETERMINATION

The microwave spectrum observed by Shoemaker[2] covered only the range frequency of 12.6−18.1 GHz and assigned many Q−branch transitions in the region as well as predicted some R−branch transitions. A higher frequency source was used in this experiment which reported more absorptions up to 26 GHz.

In order to make assignments, a spectrum was predicted for each transition using the selection rules for a μ_c transition and the rotational constants for the preferred structure D4, given by Hedberg and Hedberg. The experimentally observed transitions compared very well to the predicted output. A transition assignment for each was then made, corresponding to both Q and R− branch transitions.

Due to masking by the strong Q−branch transitions, Stark peaks for the low J, R−branch transitions ($\Delta J = 0$) were difficult to measure, even with strong absorption peaks. The transition at 14049 MHz gave the most reliable result for the determination of μ because it was the only low J transition not affected by the Q−branches. Data could not be recorded above 125V as the Stark peaks were beginning to spread. R−branch transitions are expected to show J+1 transitions where the transition with the largest displacement represents the Stark component with the highest M value. As this was a 1 ----> 2 transition, two Stark peaks were expected corresponding to M=0 and M=1. No data was recorded for the M = 0 transition because the Stark shift was almost insignificant and could not be separated from the absorption line. Data recorded for the M= 1 transition was found to be close to that predicted by the Stark shift equation (see Table 6) . Data for all assigned transitions are shown in Table 7.

Table 6

Data for the Stark Effect of the Transition at 14049.225 MHz

J = 1(0,1) ------> 2(1,1)

Voltage (V)	Electric field, ϵ (V/cm)	$\Delta\nu$ (MHz)
26	88	1.091
50	155	2.406
75	224	4.082
100	294	6.283
125	363	9.570

Table 7

Assigned Transitions for SOF_4

Transition	Calc. Freq (MHz), ν_c	Obs. Freq (MHz), ν_o	$\nu_o - \nu_c$
$*12_{7,6} - 12_{6,6}$	12075.134	12075.580	0.446
$*29_{7,22} - 29_{6,24}$	12119.128	12120.180	1.052
$*30_{8,22} - 30_{7,24}$	13231.116	13231.110	−0.006
$*31_{8,23} - 31_{7,25}$	13247.603	13239.690	−7.913
$*29_{8,21} - 29_{7,23}$	13257.231	13257.357	0.126
$28_{8,20} - 28_{7,22}$	13305.551	13305.645	0.094
$27_{8,19} - 27_{7,21}$	13366.675	13366.722	0.097
$36_{9,28} - 36_{8,28}$	13394.126	13399.164	5.038
$26_{8,18} - 26_{7,20}$	13433.653	13433.721	0.068
$25_{8,17} - 25_{7,19}$	13501.566	13501.674	0.108
$24_{8,16} - 24_{7,18}$	13567.120	13567.286	0.166
$23_{8,15} - 23_{7,17}$	13628.270	13628.406	0.136
$*32_{7,25} - 32_{6,27}$	13631.672	13631.634	−0.380
$22_{8,14} - 22_{7,16}$	13683.893	13683.996	0.103

Transition	μ_c (MHz)	μ_o (MHz)	$\Delta\nu$
$*21_{7,14}-21_{8,14}$	13723.738	13725.900	2.162
$21_{8,13} - 21_{7,15}$	13733.517	13733.568	0.051
$20_{8,12} - 20_{7,14}$	13777.109	13777.353	0.244
$19_{8,11} - 19_{7,13}$	13814.907	13815.006	0.099
$18_{8,10} - 18_{7,12}$	13847.309	13847.373	0.064
$17_{8,9} - 17_{7,11}$	13874.791	13874.892	0.101
$16_{8,8} - 16_{7,10}$	13897.857	13897.968	0.111
$15_{8,7} - 15_{7,9}$	13917.006	13917.432	0.426
$14_{8,6} - 14_{7,8}$	13932.717	13932.978	0.261
$13_{8,5} - 13_{7,7}$	13945.438	13945.869	0.431
$12_{8,4} - 12_{7,6}$	13955.582	13955.880	0.298
$11_{8,3} - 11_{7,5}$	13963.530	13963.797	0.267
$10_{8,2} - 10_{7,4}$	13969.627	13969.596	−0.031
$9_{8,1} - 9_{7,3}$	13974.188	13974.465	0.277
$8_{8,0} - 8_{7,2}$	13977.496	13977.684	0.188

Transition	μ_c (MHz)	μ_o (MHz)	$\Delta\nu$
$*{}^{2}{}_{1\,1} - {}^{1}{}_{0\,1}$	14050.588	14049.225	−1.363
$35_{9,26} - 35_{8,28}$	14813.210	14809.719	−3.491
$34_{9,25} - 34_{8,27}$	14851.564	14851.686	0.122
$33_{9,24} - 33_{8,26}$	14915.607	14915.682	0.075
$32_{9,23} - 32_{8,25}$	14992.350	14992.320	−0.030
$*31_{9,22} - 31_{8,24}$	15069.364	15074.892	5.528
$30_{9,21} - 30_{8,23}$	15158.313	15158.319	0.006
$29_{9,20} - 29_{8,22}$	15239.267	15239.361	0.094
$28_{9,19} - 28_{8,21}$	15315.629	15315.681	0.052
$27_{9,18} - 27_{8,20}$	15386.181	15386.178	−0.003
$26_{9,17} - 26_{8,19}$	15450.352	15450.549	0.197
$25_{9,16} - 25_{8,18}$	15508.011	15508.452	0.441
$*24_{9,15} - 24_{8,17}$	15559.316	15556.568	−2.748
$23_{9,14} - 23_{8,16}$	15604.595	15604.656	0.061
$22_{9,13} - 22_{8,15}$	15644.269	15644.265	−0.009
$21_{9,12} - 21_{8,14}$	15678.801	15678.822	0.033

Transition	μ_c (MHz)	μ_o (MHz)	$\Delta\nu$
$^{20}_{9,11} - {}^{20}_{8,13}$	15708.492	15708.696	0.204
$^{19}_{9,10} - {}^{19}_{8,12}$	15734.308	15734.346	0.038
* $^{2}_{2,0} - {}^{1}_{1,0}$	15754.969	15755.058	0.089
$^{18}_{9,9} - {}^{18}_{8,11}$	15756.177	15756.144	−0.003
*$^{17}_{1,17} - {}^{17}_{2,15}$	15767.415	15766.188	−1.227
$^{17}_{9,8} - {}^{17}_{8,10}$	15774.678	15774.642	−0.036
$^{16}_{9,7} - {}^{16}_{8,9}$	15790.191	15790.254	0.063
$^{15}_{9,6} - {}^{15}_{8,8}$	15803.070	15803.181	0.111
$^{14}_{9,5} - {}^{14}_{8,7}$	15813.638	15813.765	0.127
$^{13}_{9,4} - {}^{13}_{8,6}$	15822.197	15822.324	0.127
*$^{12}_{9,3} - {}^{12}_{8,5}$	15829.022	15828.969	−0.053
$^{11}_{9,2} - {}^{11}_{8,4}$	15834.367	15834.372	0.005
$^{10}_{9,1} - {}^{10}_{8,3}$	15838.463	15838.668	0.205
$^{9}_{9,0} - {}^{9}_{8,2}$	15842.543	15841.653	−0.890
*$^{27}_{5,22} - {}^{27}_{4,24}$	15844.768	15847.180	2.412
*$^{36}_{10,26} - {}^{36}_{9,28}$	16683.015	16681.070	−1.945

Transition	μ_c (MHz)	μ_o (MHz)	$\Delta\nu$
$^{31}_{10,21} - {}^{31}_{9,23}$	17140.807	17140.941	0.134
$^{30}_{10,20} - {}^{30}_{9,22}$	17212.060	17212.362	0.302
$^{29}_{10,19} - {}^{29}_{9,21}$	17271.326	17272.194	0.868
$^{28}_{10,18} - {}^{28}_{9,20}$	17334.530	17334.600	0.070
$^{25}_{10,15} - {}^{25}_{9,17}$	17473.542	17473.428	−0.114
$^{24}_{10,14} - {}^{24}_{9,16}$	17509.688	17509.830	0.142
$^{23}_{10,13} - {}^{23}_{9,15}$	17541.453	17541.564	0.111
$^{22}_{10,12} - {}^{22}_{9,14}$	17569.237	17569.317	0.080
$^{21}_{10,11} - {}^{21}_{9,13}$	17593.413	17593.536	0.123
$*^{20}_{10,11} - {}^{20}_{9,11}$	17613.319	17612.700	−0.619
$^{20}_{10,10} - {}^{20}_{9,12}$	17614.330	17614.470	0.140
$^{19}_{10,9} - {}^{19}_{9,11}$	17632.313	17632.302	−0.011
$^{18}_{10,8} - {}^{18}_{9,10}$	17647.663	17647.704	0.041
$^{17}_{10,7} - {}^{17}_{9,9}$	17660.661	17660.682	0.021
$^{16}_{10,6} - {}^{16}_{9,8}$	17671.568	17671.593	0.025

Transition	μ_c (MHz)	μ_o (MHz)	$\Delta\nu$
$^{15}_{10,5} - {}^{15}_{9,7}$	17680.626	17680.788	0.162
$^{14}_{10,4} - {}^{14}_{9,6}$	17688.059	17688.102	0.043
$^{13}_{10,3} - {}^{13}_{9,5}$	17694.076	17694.198	0.122
$^{12}_{10,2} - {}^{12}_{9,4}$	17698.870	17698.833	−0.037
$^{11}_{10,1} - {}^{11}_{9,3}$	17702.619	17702.565	−0.054
$^{10}_{10,0} - {}^{10}_{9,2}$	17705.486	17705.397	−0.089
$*^{3}_{1,2} - {}^{2}_{0,2}$	20673.887	20673.912	0.025
$*^{3}_{2,1} - {}^{2}_{1,1}$	22189.658	22189.864	0.206
$*^{3}_{2,2} - {}^{2}_{1,2}$	22412.540	22412.640	0.100

Transitions preceded by asterisks are those assigned from this experiment, others by Shoemaker

From the asymmetric rotor program, the Stark shift equation

$$\Delta\nu = (A + B\,M^2)\,\mu^2\,\epsilon^2$$

was solved for M = 1 to give $\Delta\nu = 7.1426 \times 10^{-5}\ \mu^2\epsilon^2$. A plot of $\Delta\nu$ versus ϵ^2 was then made giving a slope = 6.7×10^{-5} with R = 0.9996. From this output, μ was then determined as 0.97 ± 0.02 Debye. Figure 13 shows the graph of $\Delta\nu$ versus ϵ^2 for this transition.

For the Q−branch transitions ($\Delta J = 0$) the Stark peak observed was a composite of all Stark components from M = 1 ----> M = M_{max} because the Stark separation for the M values were very small and therefore close to each other. A reliable data for μ could therefore not be determined.

From the bond angle and bond length data an MOI program[15] to calculate the moments of inertia, I_a, I_b and I_c and the rotational constants, A, B, C, for each proposed structure was run. These are shown in Table 1. A nonlinear least squares fit[16] was performed on the observed frequencies in order to check the validity of the assignments and determine the rotational constants. The fit was non linear because there were very few R− branch data in the region studied. The calculated rotational constants for the proposed electron diffraction structures were then compared to determine which values were closest to those obtained from the microwave data.

The least squares fit was performed using 132 observed transitions and the output gave values of A, B and C that were very close to those proposed for structure D4 by HH (See Table 8). The comparative values are:

	Least Squares Fit (MHz)	HH Model D4 (MHz)	Δ (MHz)
A	4181.0 ± 0.04	4179.1	−1.9
B	3289.8 ± 0.04	3291.4	1.6
C	3206.3 ± 0.04	3209.1	2.8

A complete set of the data is shown in Table 9.

Substitution of A, B, and C back into equations (2), (3) and (4) respectively, gave the moments of inertia, in units of amu $\mathring{A}^2$, to be:

$I_a = 120.874$ $\quad I_b = 153.620$ $\quad I_c = 157.622$

SOF_4

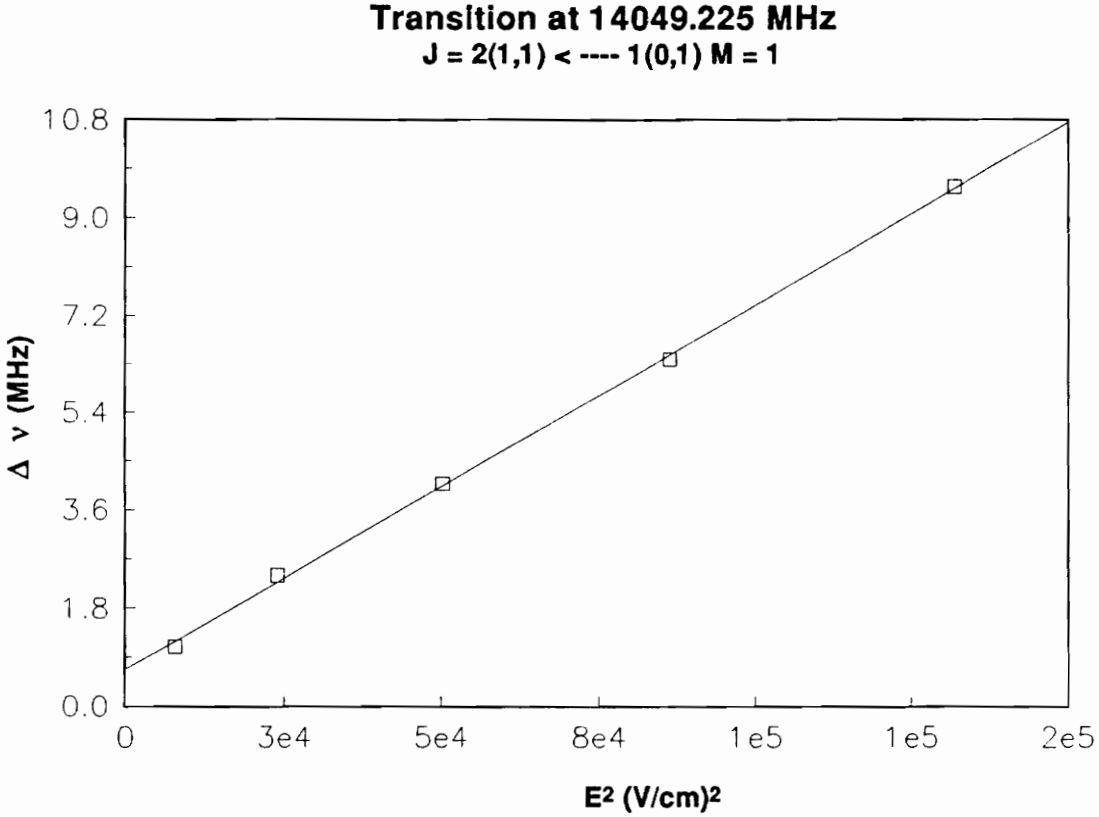

Figure 13: $\Delta\nu$ vs ϵ^2 for the transition at 14049 MHz

Table 8

Derived Rotational Constants for Thionyl Tetrafluoride

Rotational Constant	GH[1]-A	GH-B	GH-C	GH-D	HCB[2]-I	HCB-II	HH[3]-D4	LSF[4]
A	4145.3	4146.5	4174.0	4199.9	4118.5	4139.9	4179.1	4181.0
B	3376.5	3269.5	3384.3	3327.3	3375.4	3239.6	3291.4	3289.8
C	3130.3	3243.9	3142.3	3189.0	3098.3	3229.9	3209.1	3206.3

1 = Gunderson and Hedberg[8](Structures A, B, C, D)

2 = Hencher, Cruickshank and Bauer[6]

3 = Hedberg and Hedberg[9]

4 = Least Squares Fit

Table 9

Parameters Derived from the Least Squares Fit of 132 Transitions (MHz)

A	=	4181.0 ± 0.04
B	=	3289.9 ± 0.04
C	=	3206.3 ± 0.04
Tau(1)	=	−0.034 ± 0.04
Tau(2)	=	−0.011 ± 0.04
Tau(3)	=	1.980 ± 1.59
T(AAAA)	=	−0.012 ± 0.01
T(BBBB)	=	−0.013 ± 0.01
T(CCCC)	=	−0.012 ± 0.01
HJ	=	1.308 E−05 ± 6.23 E−05
HJK	=	−1.768 E−09 ± 6.23 E−09
HKJ	=	−2.453 E−08 ± 5.68 E−08
HK	=	−3.529 E−07 ± 1.90 E−07
H'J	=	0
H'JK	=	0
H'K	=	0

A rigid rotor fit performed on the low J transitions where centrifugal distortion is minimal and the data output gave

$$A = 4181.0 \pm 0.02; \quad B = 3289.8 \pm 0.02; \quad C = 3206.2 \pm 0.02.$$

Since the constants from the rigid rotor data are so close to the least squares fit data, it confirms that centrifugal distortion was minimal for this molecule.

SUMMARY

Earlier investigations of SOF_4 proposed various models, all of which gave reasonable fits to the electron diffraction data. Further investigation by HH[9] gave preference to the D over the B type models when vibrational effects were considered. From the data by HH a microwave investigation was undertaken to confirm a structure as well as determine the dipole moment of SOF_4.

The experimental spectrum exhibited strong, high J, Q−branch transitions which masked the low J, R−branch transitions, even at low voltages. Also, spectra could not be recorded below 25 volts because only a very low gas pressure could give lines narrow enough for resolution and then there was not enough sample in the cell to make a detection.

The experimental spectrum was in good agreement with that calculated using the least squares fitting method and the rotational constants were determined, in units of MHz, to be:

$$A = 4181.0 \pm 0.04 \qquad B = 3289.790 \pm 0.04 \qquad C = 3206.255 \pm 0.04$$

The determined moments are closest to those proposed for the electron diffraction structure D4 by HH[9] as shown in Table 8. The values are not expected to be identical because the moments derived from electron diffraction are actually from a vibrationally averaged structure; on the other hand, microwave spectroscopy observes only a specific vibrational state for the molecule, in this case a ground state. In addition, the closeness of the least squares fit for 132 transitions was sufficiently good to confirm that the microwave work of Murty[10] was incorrect.

The dipole moment was estimated from the shift of the composite Stark peak for several high J, Q−branch transitions to be 1.1 Debye. A more detailed analysis of the R−branch transition at 14049 MHz gave a dipole moment of 0.97 Debye. Unfortunately, this was the only low J line that was not substantially masked by Q−branch transitions. Therefore the dipole moment could not be confirmed from any other low J transition .

To completely determine the structure of SOF_4, three additional moments of inertia, need to be measured. This can be accomplished through a microwave study of the isotopically substituted ^{34}S species.

REFERENCES

1. Kimura, K. and Bauer, S. H., *J. Chem. Phys.*, 39, 3172 (1963).

2. Shoemaker, C. Ph.D. Dissertation, VPI&SU, (1973), "Molecular Structure Investigation of Chromyl Fluoride, Bis (Trifluoromethyl) Nitroxide, and Sulfur Oxide Tetrafluoride."

3. Graybeal, J. D. (unpublished data)

4. Goggin, P. L., Roberts, H. L., and Woodward, H. L., *Trans. Faraday Soc.*, 57, 1877 (1961).

5. Tolles, W. M., and Gwinn, W. D., *J. Chem. Phys.*, 36, 1119 (1962).

6. Hencher, J. L., Cruickshank, D. W. J., and Bauer, S. H., *J. Chem. Phys.*, 48, 518 (1968).

7. Gillespie, R. J., *J. Chem. Phys*, 37, 2498 (1962).

8. Gundersen, G. and Hedberg, K., *J. Chem. Phys.*, 51, 2500(1969).

9. Hedberg, L. and Hedberg, K., *J. Chem. Phys.*, 86, 598 (1982).

10. Murty, K.S.R., *Bull. Nat. Inst. Sci. India*, 30, 73 (1965)

11. Townes, C. H. and Schalow, A. L., Microwave Spectroscopy, McGraw-Hill Book Co., Inc., New York (1970).

12. Gordy, W., and Cook, R. L., Microwave Molecular Spectra, Vol. XVIII, John Wiley and Sons, New York (1984).

13. Wang, S. C., *Phys Rev.*, 34, 243 (1929).

14. Beaudet, R. A. , Ph.D. Dissertation, Harvard University, (1962)"Asymmetric Rotor Program to determine calculated frequencies."

15. Beaudet, R. A., and Pauly, W. R., MOI: Fortran Program for the calculation of the moments of inertia of molecules from the bond distances and angles.

16. Kirchoff, W.H., (1972), "On the Calculation and Interpretation of Centrifugal Distortion Constants.: A Statistical Basis for Model Testing: The Calculation of the Force Field."

APPENDIX I: PROGRAM FOR THE CALCULATION OF LINE SHAPES

```
public k,k1,delnu_k,nu_j1,nu_0k,delnu_ki,ax,bx,a1k,b1k
SET STATUS On
SELECT 1
USE DIPOLE

SELECT 2
USE ELECTRIC

@ 12, 5 SAY " CALCULATION OF A LINE SHAPE THROUGH FREQUENCY VARIATION"
@13,5                                                                    SAY
"_____________________________________________________________________
"
?
WAIT
CLEAR

***INPUT DATA VALUES
k =  0
k1 = 0
A1k = 0
B1k = 0
ax=0
bx=0
delnu_k = 0
nu_0k = 0
delnu_ki = 0
@  6, 2 say "k = " get k PICTURE "99"
@  6,27 say "k1 = " get k1 PICTURE "99"
@  9, 2 say "Ak = " get A1k picture "99.9999"
@  9,15 say "e" get ax picture "999"
@  9,25 say "Bk = " get B1k picture "99.9999"
```

```
@  9,38 say "e" get bx picture "999"
@ 12, 2 say "nu_0k = " get nu_0k PICTURE "999999.999"
@ 12,25 say "delnu_k = " get delnu_k PICTURE "99.999"
@ 12,47 say "delnu_ki = " get delnu_ki PICTURE "99.999"
READ
Ak=A1k*10**ax
Bk=B1k*10**bx
MCOUNT = 1
SELECT 1

***INCORPORATE DIPOLE (MU) VALUE
DO WHILE .NOT. EOF()
   MU = MU1
   SELECT 3
   ME = 'OUT' + STR(MCOUNT,1)
   me1=me+".dbf"
   jo=0
   ! copy &me1 c:
   me2="c:"+me1
   me3=substr(me2,1,6)
   USE &ME3
   SELECT 2
   go top

***INCORPORATE ELECTRIC FIELD (E)
   ECOUNT = 1
   DO WHILE .NOT.EOF()
      ? ecount
      E = E1
      FLD = 'OTPT' + STR(ECOUNT-1,1)
      fld1='freq'+str(ecount-1,1)
      SELECT 3
***DETERMINE NU_J1
```

```
      IF (Ak >= 0) .and. (Bk >= 0)
         nu_J1 = nu_0k+((Ak+(Bk*(k**2)))*(mu**2)*(E**2))
      ELSE
         M = 0
         nu_J1 = 0
         DO WHILE M <= k
            M1 = nu_0k+((Ak+(Bk*(M**2)))*(mu**2)*(E**2))
            nu_J1 = IIF(M1 > nu_J1, M1, nu_J1)
            M = M + 1
         ENDDO
      ENDIF
      Lrange = nu_0k - (4*delnu_k)
      Rrange = nu_J1 + (4*delnu_k)
      nu_j = Lrange
      Rrange = IIF (nu_0k > Rrange, nu_0k, Rrange)

***DETERMINE STEP SIZE
      step = (Rrange - Lrange) / 300
     bo=0
      DO WHILE nu_j <= Rrange
         i = 1
         I_k = 0
         tot = 0
         DO WHILE i <= (k+1)
            M_ki = i - 1
            IF k = k1
               L_ki = M_ki ** 2
            ELSE
               L_ki = ((k+1) ** 2) - (M_ki ** 2)
            ENDIF
            I_k = L_ki + I_k
            nu_ikl=nu_0k+((Ak+(Bk*(M_ki**2)))*(mu**2)*(E**2))
            S_ikl=(L_ki*delnu_ki)/((delnu_ki**2)+(nu_j-nu_ikl)**2 )
```

```
            tot = tot + S_ikl
            i = i + 1
         ENDDO
         S_0k = (I_k * delnu_k) / ((delnu_k ** 2)+;
            (nu_j - nu_0k) ** 2)
         S_kl = S_0k - tot
         nu_j = nu_j + step
         IF bo=jo
            APPEND BLANK
            jo=jo+1
            bo=bo+1
            REPLACE &FLD WITH S_kl, &fld1 with nu_j
         ELSE
            REPLACE &FLD WITH S_kl, &fld1 with nu_j
            bo=bo+1
            SKIP
         ENDIF
      ENDDO
      GO TOP
      ECOUNT = ECOUNT + 1
      SELECT 2
      SKIP
   ENDDO
   select 3
   use
   ! copy &me2 b:
   ! del &me2
   MCOUNT = MCOUNT + 1
   SELECT 1
   SKIP
ENDDO
```

VITA

Patricia Fida Webber was born on December 17, 1964 in Kenema Sierra Leone. She received her Bachelor of Science degree in Chemistry from Stockton State College in Pomona, New Jersey. In 1987, she entered Virginia Polytechnic Institute and State University to pursue a Master of Science degree in Chemistry.